

## Constructability optimal design of reinforced concrete retaining walls using a multi-objective genetic algorithm

A. Kaveh\*, M. Kalateh-Ahani and M. Fahimi-Farzam

*Centre of Excellence for Fundamental Studies in Structural Engineering, School of Civil Engineering,  
Iran University of Science and Technology, Narmak, Tehran-16, Iran*

*(Received January 2, 2013, Revised July 15, 2013, Accepted July 17, 2013)*

**Abstract.** The term “constructability” in regard to cast-in-place concrete construction refers mainly to the ease of reinforcing steel placement. Bar congestion complicates steel placement, hinders concrete placement and as a result leads to improper consolidation of concrete around bars affecting the integrity of the structure. In this paper, a multi-objective approach, based on the non-dominated sorting genetic algorithm (NSGA-II) is developed for optimal design of reinforced concrete cantilever retaining walls, considering minimization of the economic cost and reinforcing bar congestion as the objective functions. The structural model to be optimized involves 35 design variables, which define the geometry, the type of concrete grades, and the reinforcement used. The seismic response of the retaining walls is investigated using the well-known Mononobe-Okabe analysis method to define the dynamic lateral earth pressure. The results obtained from numerical application of the proposed framework demonstrate its capabilities in solving the present multi-objective optimization problem.

**Keywords:** reinforced concrete cantilever retaining wall; constructability; reinforcing bar congestion; multi-objective optimization; non-dominated sorting genetic algorithm

---

### 1. Introduction

The economy of a reinforced concrete (RC) construction project does not depend only on the amount of concrete and steel used or the formwork cost, rather a poor constructability of the design may affect greatly the overall cost of the project. High steel congestion makes both steel and concrete placement difficult, which delays the construction time at the site, and consequently, imposes unforeseen costs to the project due to the interruptions occur during the project completion. On the other hand, a poor constructability deteriorates the integrity of concrete and steel, which has a significant impact on the ductility of the structure. Therefore, in order to achieve an actual optimal design of a RC structure, constructability should also be considered as one of the desired objectives in the optimization procedure. Undoubtedly, this is also true in the optimal design of RC retaining walls.

Retaining walls constitute an integral part of the infrastructure that are frequently constructed for a variety of applications, most commonly for bridge abutments, roads, transportation systems, lifelines and other constructed facilities. Design of retaining walls should address at least two basic

---

\*Corresponding author, Ph.D. Student, E-mail: [alikaveh@iust.ac.ir](mailto:alikaveh@iust.ac.ir)

requirements: “stability”, which means the structure as a solid should retain the backfill mass with respect to geotechnical requirements, and “strength”, which is ensured by providing sufficient resistance against bending moments and shear forces prescribed by structural concrete codes (Das 2010). Another key factor for the optimal design of walls is the inclusion of a limitation on the deflections at the top of the wall. This serviceability check is performed to avoid excessively flexible walls that are not appropriate for practical purposes (Yepes *et al.* 2008).

An economic optimization of RC retaining walls has been conducted in several studies. Saribas and Erbatur (1996) applied a nonlinear programming method to solve a seven design variables problem. Ceranic *et al.* (2001), for the same size problem, utilized simulated annealing to minimize the costs. Yepes *et al.* (2008) performed a parametric study with simulated annealing for optimum RC retaining walls by formulating the problem containing 20 design variables. Harmony search and charged system search algorithm with seven design variables were adopted by Kaveh and Shakouri-Mahmud-Abadi (2010) and Kaveh and Behnam (2012) as the optimization algorithms, respectively. Minimizing the embedded carbon dioxide emissions was studied by Yepes *et al.* (2012) through employing a variable neighborhood search strategy, based on their previous work in 2008. CO<sub>2</sub> optimization was also considered by Khajezadeh *et al.* (2013), using a gravitational search algorithm for a structural model with eight design variables.

This paper presents a new framework for optimal design of RC cantilever retaining walls, consisting of two objective functions that are the reinforcing bar congestion and the economic cost. The meta-heuristic utilized here is NSGA-II, a popular, fast sorting and elitist multi-objective genetic algorithm (Deb *et al.* 2002). The wide application of this algorithm in engineering problems proves its great abilities in covering the Pareto front and solving the multi-objective optimization problems (Kaveh *et al.* 2012). Its particular fitness assignment scheme consists of sorting the population in different fronts using the non-domination order relation. Solutions which dominate other solutions receive higher rank value and are preferred to generate the next generation. In order to form the next generation, the algorithm combines the current population and its offsprings generated with the crossover and mutation operators. Finally, the best individuals in terms of non-dominance and diversity are chosen (Deb *et al.* 2002). In this research, a new version of polynomial mutation for discrete representation is developed using basic and simple concepts, which will be fully explained in Section 5.

In the model established for the structure, to provide more practical designs applicable in real-world constructions, 35 design variables are considered consisting of seven geometric, two material types, and 26 variables for reinforcement setup. A structural evaluation module is developed to check all the relevant geotechnical and structural requirements needed to be considered according to (AASHTO 2002) and (ACI 318-08) specifications for the design of common RC retaining walls. In this paper, for improving the robustness of the proposed method, the seismic response of the retaining walls is also investigated during the analysis process.

Excessive dynamic lateral earth pressure on retaining structures resulting from earthquakes has caused several major damages in the past. The increase of lateral earth pressure during earthquakes induces sliding and/or overturning to the retaining walls. The dynamic response of even simplest type of retaining wall is quite complex. Wall movement and pressure depends on the response of the soil underlying the wall, the response of the backfill, the inertial and flexural response of the wall itself, and the nature of the input motions (Das *et al.* 2010). Here, we adopt one of the methods widely used by most of the design engineers for determining the dynamic lateral pressure on retaining structures that has been developed by Okabe (1926) and Mononobe (1929). This method is generally referred to as the “Mononobe-Okabe analysis”, recommended by AASHTO

(2002) for seismic evaluations of retaining structures. Mononobe-Okabe method considers pseudo-static approach. In recent years, some studies conducted on developing pseudo-dynamic procedures, e.g., Giri (2011) used a pseudo-dynamic method to compute the distribution of seismic earth pressure on a rigid cantilever retaining wall supporting dry cohesionless backfill.

After this opening section, the paper is organized as follows: Section 2 explains the optimization problem and its objective functions; section 3 concerns structural modeling and defines the design variables; in Section 4, the structural evaluation module and constraints of the problem are formulated; section 5 briefly introduces the NSGA-II; the proposed framework is presented in Section 6; numerical results on design of a typical RC retaining wall of 8 m in height and 100 m in length are investigated in Section 7 and finally the paper is concluded with Section 8.

## 2. Optimal design problem

The present optimization problem deals with a bi-objective optimization of the economic cost and reinforcing bar congestion of the RC retaining walls. This can be expressed as

$$\begin{cases} \text{minimize } F(x) = (\text{Cost}(x), \text{Congestion}(x)) \\ g_i(x) \leq 0 \quad i = 1, 2, \dots \end{cases} \quad (1)$$

where  $x = \{x_1, x_2, \dots, x_n\}$  are the design variables and  $g(x)$  represents all the constraints and requirements that the structure must satisfy according to the design codes. The first objective function as defined by Eq. (2), is the economic cost of the structure, where  $p$  are the unit prices,  $m$  measures the steps the construction process of a common RC retaining walls is divided into, and  $r$  is the total number of these steps. The cost function comprises of the cost of materials (concrete and steel) and the cost of all construction steps required to evaluate the entire cost of the wall per meter of length, e.g., formworking, earth removal, backfill and concrete placing. The unit prices considered for the construction steps are given in Table 1. These prices were provided by a local Iranian contractor of road construction in November 2012.

$$\text{Cost} = \sum_{i=1}^r p_i \times m_i \quad (2)$$

Optimization of concrete structures based only on cost often results in structures whose constructability is poorly treated, since results tend to reinforcement arrangements with close spacings of small diameter bars. In this sense, the number of bars is regarded as an indicator of reinforcing steel congestion. Fewer bars involve larger diameters with greater spacings, leads to better constructability, since lower bar congestion implies fewer execution errors, less complex quality controls and faster construction processes (Martinez-Martin *et al.* 2012). The second objective function computes the total number of bars in the structure as

$$\text{Congestion} = \sum_{i=1}^k n_i \quad (3)$$

where  $n_i$  is the number of bars of the  $i$ th reinforcement set per meter length of the wall, calculated by dividing the corresponding bar spacing from the dimension that is distributed along. Different

Table 1 Unit prices of the construction steps

| Unit  | Cost (US\$) |
|---|-------------|
| Cubic meter of earth removal                  | 11.41       |
| Cubic meter of backfill                       | 38.1        |
| Kilogram of steel (4000 kg/cm <sup>2</sup> )* | 1.54        |
| Kilogram of steel (3000 kg/cm <sup>2</sup> )  | 1.51        |
| Cubic meter of concrete (20 MPa)*             | 94.45       |
| Cubic meter of concrete (25 MPa)              | 99.49       |
| Cubic meter of concrete (30 MPa)              | 104.51      |
| Cubic meter of concrete (35 MPa)              | 108.53      |
| Cubic meter of concrete (40 MPa)              | 118.05      |
| Square meter of foundation formwork           | 36.82       |
| Square meter of stem formwork                 | 37.08       |
| Cubic meter of concrete placing               | 35.48       |

\*For steel materials indicates the specified yield strength and for concrete materials indicates the compressive strength.

reinforcement sets may be considered for the common RC retaining walls, such as bending and shear reinforcement or secondary reinforcement for shrinkage and thermal effects;  $k$  is the total number of reinforcement sets in the structure.

### 3. Structural modeling

The model of the structure comprises of 35 design variables, which define the geometry, the type of concrete grades, and the reinforcement used. The geometric properties and the reinforcement setup of the developed model is shown in Fig. 1. Design variables includes 7 geometric values, i.e., bottom thickness of the stem  $w_{bottom}$ , thickness of the base slab  $h_{slab}$ , length of the heel  $w_{heel}$ , length of the toe  $w_{toe}$ , thickness of the shear key  $w_{key}$ , depth of the shear key  $h_{key}$ , and location of the shear key  $b_{key}$ . The top thickness of the stem  $w_{top}$  is assumed to be constant. As well, two variables indicate the concrete grades used in the stem and the base slab, respectively. The strength of a concrete mix is measured in grades that the grade of concrete means the concrete compression resistance after 28 days ( $f_c$ ).

The remaining 26 variables describe the reinforcement setup, which includes two groups of variables. One group represents the bar diameters of the reinforcement sets containing 15 variables, and the other defines the spacings between the bars with 11 variables. Different reinforcement sets are considered in the model developed for the structure in different parts of the stem and the base slab, demonstrated in Fig. 1(b). In this figure, each reinforcement set is identified by two types of variables, one indicating the diameter of the bars ( $D$ ), and the other the spacing of them ( $S$ ). The difference between the number of variables assigned to the diameters and the spacings is for the attention to the ease of reinforcement placing, since it is desirable that the extra bars are bundled together with the existing bars. In Fig. 1(b), the reinforcement sets have the same spacing are specified by the identical spacing variable number. As each reinforcement set has a specific variable for its bars diameter, hereinafter, the reinforcement sets are denoted by the number of their  $D$  variable.

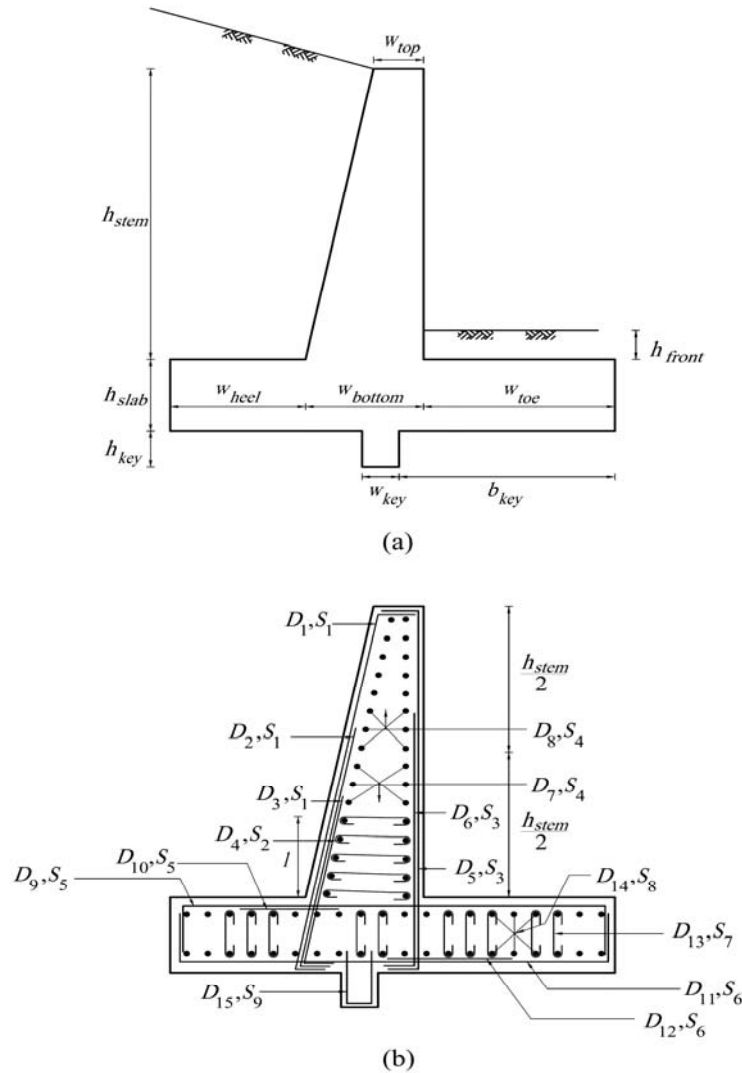


Fig. 1 The model developed for RC retaining walls; (a) geometric properties, (b) reinforcement setup

Vertical flexural steel includes three sets of reinforcement bars for the bending of the stem (variables  $D_1$ ,  $D_2$  and  $D_3$ ). Lengths of these bars are 100, 50 and 25% of the height of the stem, respectively. Shear reinforcement in the stem is specified by variable  $D_4$ , which is the diameter of reinforcement from the bottom of the stem up to a height  $l$ . This height is where the concrete shear capacity is sufficient to carry the applied shear force, so that there is no need for further reinforcement. In this study, as illustrated in Fig. 1(b), tie bars are used as the shear reinforcement in both the stem and the base slab. Variables  $D_5$  and  $D_6$  are the vertical and variables,  $D_7$  and  $D_8$  are the longitudinal secondary reinforcements that are inserted in the stem to avoid shrinkage and thermal effects. Lengths of the reinforcement  $D_5$  and  $D_6$  are equal to the total and half-height of the stem, whereas reinforcement  $D_7$  and  $D_8$  are distributed longitudinally through top half and bottom half of the stem, respectively.

Bending bars in the base slab include variables  $D_9$  and  $D_{10}$  for the heel and  $D_{11}$  and  $D_{12}$  for the toe. Reinforcement  $D_9$  and  $D_{11}$  are the bars of the total width of the base slab and length of the reinforcement  $D_{10}$  and  $D_{12}$  are equal to the half-length of the heel and the toe, respectively. Shear reinforcement in the base slab is expressed by variable  $D_{13}$ , whereas variable  $D_{14}$  corresponds to the secondary reinforcement. Variable  $D_{15}$  represents the bending reinforcement in the shear key. Thus far, 15 reinforcement sets with a total of 15 variables for the bar diameters and 9 variables for the spacings are defined. The numbering of these variables is shown in Fig. 1(b). The last two variables of the spacings group denote the number of shear bars in the stem and the base slab per meter length of the wall. The allowable values for these two variables are 3, 4, 5, 8, and 10 that correspond to 33, 25, 20, 15, and 10 cm spacing of the tie bars, respectively.

In conventional design procedures, the required reinforcement areas are taken as the variables. Hence for determining the reinforcement setup, the designer just needs to select an allowable value for either the diameter or spacing of the bars, the other one is computed subsequently. However in this study, both diameter and spacing of the bars are considered to be variable that follows two purposes. (1) Automation: in this approach all values needed to define the reinforcement setup, are determined in the optimization procedure and not by the designer. (2) Diversification: in the constructability optimization, this approach makes the heuristic search more diversified, since in the conventional procedures, the interference of the designer perhaps confines the solutions that can be generated.

To complete the structural modeling, in addition to the presented design variables, some parameters should be determined. The parameters of a typical RC retaining wall are all of the magnitudes taken as fixed data, consisting of some geometric values, properties of the base soil and backfill, and some design specifications, which will be introduced in the subsequent sections.

#### 4. Structural evaluation module

In the optimization program, after modeling the structure in terms of the design variables, a structural evaluation module needed to analyze the structure and check all the design constraints. Structures that meet all the constraints are called feasible solutions, and those that do not are unfeasible ones.

There are two phases in the design of a common RC retaining wall. First, with the lateral earth pressure being known, the structure as a whole is checked for “stability” under the service loads, i.e., the structure is examined for possible “overturning”, “sliding”, and “bearing capacity” failures. Second, each component of the structure is checked for “strength” under the combined factored loads, and the required steel reinforcement of each component is verified. In what follows, a brief summary for determining the stability of the retaining walls is presented; checks for strength can be found in any text book on reinforced concrete. For more information on the terminology and details, interested readers may refer to Das (2010).

The seismic behavior of retaining walls depends on the total lateral earth pressure that develops during the earth shaking. This total pressure includes both the static gravitational pressure that exist before earthquake occurs and the transient dynamic pressure induced by the earthquake. AASHTO (2002) specifies that, for the analysis of the retaining walls, the pseudo-static Mononobe-Okabe analysis method is to be used. Fig. 2 demonstrates the key forces considered in the Mononobe-Okabe solution: The weight of the concrete wall ( $W_1$ ), the weight of the backfill ( $W_2$ ), the weight of soil on the toe ( $W_3$ ), the surcharge load ( $\omega$ ), the inertial force in the horizontal

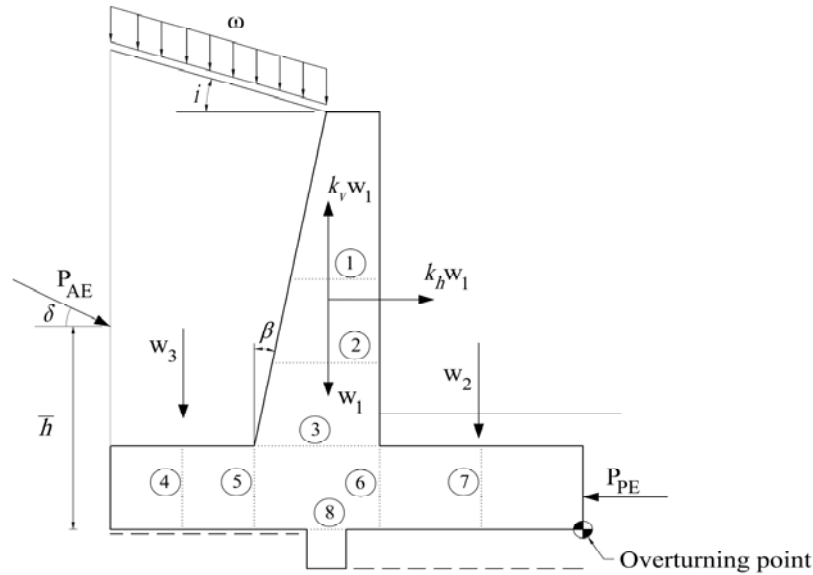


Fig. 2 Main forces in the Mononobe-Okabe solution

direction ( $k_h W_1$ ) and in the vertical direction ( $k_v W_1$ ), and finally the seismic active and passive earth pressures ( $P_{AE}$  and  $P_{PE}$ ).

The computation of  $W_1$ ,  $W_2$ , and  $W_3$  is straightforward, multiplying the unit weights by the respective volumes, applied at their center of mass. A surcharge load results from forces that are applied along the surface of the backfill behind the wall, such as an embankment load, car parking, floor load or temporary loads like construction traffic and stockpiles of material. The surcharge produces an active pressure against the wall. For considering this effect in the analysis, the uniform surface pressure may be converted to an equivalent height of fill, and then the earth active pressure is calculated for the correspondingly greater height, i.e.,  $h_{eq} = \omega/\gamma_{soil}$ , where  $\gamma_{soil}$  is the unit weight of soil and  $h_{eq}$  is the equivalent height that is added to the height of the backfill.

The Mononobe-Okabe method makes use of the acceleration coefficient (based on the geographic location of the wall), which is decomposed into horizontal and vertical components. According to AASHTO (2002) seismic specifications, for free standing retaining walls, the horizontal acceleration coefficient  $k_h$  is taken as half of the acceleration coefficient  $A$ , i.e.,  $k_h = A/2$ , and the vertical acceleration coefficient  $k_v$  is considered to be zero. The active force under seismic condition is computed as follows (Das *et al.* 2010)

$$P_{AE} = \frac{1}{2} \gamma_{soil} h^2 (1 - k_v) K_{AE} \quad (4)$$

$$K_{AE} = \frac{\cos^2(\phi - \beta - \theta)}{\psi \cos^2(\beta) \cos(\theta) \cos(\delta + \beta + \theta)} \quad (5)$$

$$\psi = \left[ 1 + \sqrt{\frac{\sin(\phi + \delta) \times \sin(\phi - \theta - i)}{\cos(\delta + \beta + \theta) \times \cos(i - \beta)}} \right]^2 \quad (6)$$

$$\theta = \arctan\left(\frac{K_h}{1 - K_v}\right) \quad (7)$$

where

$h$  = height of the backfill,

$\phi$  = internal soil friction angle,

$\beta$  = slope of rear face of the stem with respect to the vertical,

$\delta$  = angle of friction between soil and the rear face of the stem,

$i$  = the backfill slope angle with respect to the horizontal.

The force  $P_{AE}$  acts at  $\bar{h}$  from the bottom of the base slab, given by:

$$\bar{h} = \frac{P_A\left(\frac{1}{3}h\right) + \Delta P\left(\frac{2}{3}h\right)}{P_{AE}} \quad (8)$$

where  $P_A$  is the static active earth pressure defined as  $P_A = 1/2\gamma_{soil}h^2K_A$ ; assuming  $\theta$  to be zero, the formula for calculation of  $K_A$  will be the same as for  $K_{AE}$ . The dynamic passive force, using the same parameters given for the active force, is expressed as

$$P_{PE} = \frac{1}{2}\gamma_{soil}h^2(1 - k_v)K_{PE} \quad (9)$$

$$K_{PE} = \frac{\cos^2(\phi + \beta - \theta)}{\psi' \cos^2(\beta) \cos(\theta) \cos(\delta - \beta + \theta)} \quad (10)$$

$$\psi' = \left[ 1 + \sqrt{\frac{\sin(\phi + \delta) \times \sin(\phi - \theta + i)}{\cos(\delta - \beta + \theta) \times \cos(i - \beta)}} \right]^2 \quad (11)$$

As mentioned above, three constraints verify the stability of the wall for possible failures. Firstly, the stabilizing moments must be greater than the overturning moments to prevent rotation of the wall about the toe. The stabilizing moments result mainly from the self-weight of the structure and the weight of the backfill, whereas the main source of overturning moments is the seismic active earth pressure. The factor of safety against overturning is derived as

$$FS_{overturning} = \frac{\sum M_R}{\sum M_O} \quad (12)$$

where  $\sum M_O$  is sum of the moments of forces tending to overturn about the overturning point (see Fig. 2), and  $\sum M_R$  is sum of the moments of forces tending to resist overturning.

Secondly, the total horizontal reactions must be such that prevents the wall from sliding along its base. The factor of safety against sliding is calculated from

$$FS_{sliding} = \frac{\sum F_R}{\sum F_d} \quad (13)$$

where  $\Sigma F_R$  is sum of the horizontal resisting forces and  $\Sigma F_d$  is sum of the horizontal driving forces. In considering the criterion of sliding, the major driving force produced by the lateral earth pressure while the sliding resistance of retaining walls is derived from the base friction between the wall base and the foundation soil.

To increase the sliding resistance of retaining walls, other than providing a large self-weight or a large retained soil mass, shear keys can be installed at the base. The main purpose of installation of shear keys is to increase the extra passive resistance developed by the height of shear keys. Friction angle between the base and the foundation soil ( $\delta'$ ) is normally about a fraction of the angle of internal resistance, i.e.,  $\delta' < \varphi$ , where  $\varphi$  is the angle of internal friction of foundation soil. When a shear key is installed at the base of a retaining wall, the failure surface at the left side of the key is changed from the base/soil horizontal plane to a plane within the foundation soil, shown in Fig. 2 with dashed lines. Therefore, the friction angle mobilized in this case is  $\varphi$  instead of  $\delta'$  in the previous case and consequently the sliding resistance would be enhanced (Das 2010).

Finally, the bearing capacity of the foundation soil must be large enough to resist the pressures transmitted to the soil by the base slab. The factor of safety against bearing capacity failure is determined by

$$FS_{\text{bearing}} = \frac{1.33q_a}{q_{\text{max}}} \quad (14)$$

where  $q_a$  is the allowable bearing capacity of the foundation soil and  $q_{\text{max}}$  is the maximum contact pressure occurs at the end of the toe section. AASHTO (2002) permits the value of  $q_a$  used for static loading designs to be increased by 33% for the seismic loading conditions; the factor 1.33 in the numerator of Eq. (14) refers to this point. As shown in Fig. 3(a), the distribution of pressure by the base on the foundation soil is not uniform and calculated from

$$q_{\text{max}} = \frac{P}{BL} \left(1 \pm \frac{6e}{B}\right) \quad (15)$$

where  $P$  is sum of the vertical loads.  $B$  and  $L$  are the width and length of the base, respectively. The distance  $e = M/P$  is the eccentricity of the resultant of reaction forces, where  $M$  is the sum of the moments on the base slab.

In relation with the bearing capacity failure, one additional constraint is needed to check the minimum contact pressure. When the value of the eccentricity becomes greater than  $B/6$ ,  $q_{\text{min}}$  becomes negative. Thus, there will be some tensile stress at the end of the heel section. This upward pressure is not desirable because makes a part of the base to lose contact with the supporting ground during loading and consequently intensifies the potential of overturning. If the analysis of a design shows that  $e > B/6$ , then the solution is discarded.

The strength calculations of the wall are performed per linear meter for ultimate flexure and ultimate shear at different cross sections of the stem and the base in accordance with ACI 318-08. These sections are identified in Fig. 2 with dotted lines. It should be considered that the critical sections for bending moments in the base are taken at the face and back of the stem, whereas the critical sections for shear are taken at a distance  $d$  from the face of the stem for the toe and from the back of the stem for the heel section, where  $d$  is the effective depth of section. After the ultimate bending and shear capacities at the critical sections are verified, it must be checked whether the secondary reinforcement of the stem and the base comply the minimum requirements of the provisions for the thermal and shrinkage effects.

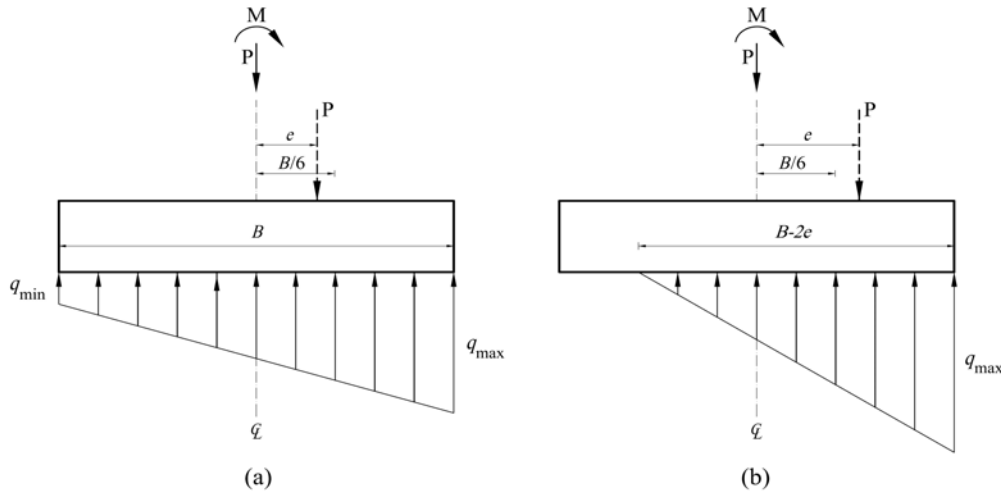


Fig. 3 Pressure distribution under an eccentrically loaded foundation; (a) when the resultant force is within the middle third of the base, (b) when the resultant force is outside the middle third of the base

For the structural design of the base slab, the distribution of ground pressure under the factored load combinations is required. Perhaps in some situations, the minimum contact pressure from Eq. (15) becomes negative, since the check for the eccentricity is done under the service loads. This means tension will develop over a length of the heel, and then there will be a separation between the base and the soil underlying it. In these situations, i.e., when  $e > B/6$ , AASHTO (2002) suggests a triangular distribution over an effective length of the base ( $B - 2e$ ) as shown in Fig. 3(b). The value of  $q_{\max}$  is obtained by

$$q_{\max} = \frac{4P}{3L(B - 2e)} \quad (16)$$

In order to avoid the problems caused by the large eccentricities, in this study, the permissible value of  $e$ , under the factored loads, is bounded to  $B/4$ .

As declared by Yepes *et al.* (2008), another important constraint which is usually ignored is a limitation on deflections at the top of the stem. Optimal design of walls without checking this serviceability limit state may lead to extremely flexible stems, not feasible for practical purposes. He reported that a limit of  $1/150$  of the stem height could be considered as an acceptable threshold level. The service load produces major deflections is the static active earth pressure, which has a triangular distribution over the height of the stem with maximum intensity of  $q_0 = KA\gamma_{\text{soil}}h_{\text{stem}}$  (see Fig. 4(a)). In this paper, we present a simple formulation for calculation of the stem deflection based on the well-known second theorem of Castigliano. This theorem states the first partial derivative of the total strain energy in a linearly elastic structure with respect to the force applied at any point is equal to the deflection at the point of application of that force in the direction of its line of action (Kaveh 2006). In a cantilever beam with a transverse loading, the flexural and shear deformations generally define the strain energy. Thus in order to compute the deflection, as shown in Fig. 4(b), it is just enough to impose a dummy concentrated force at the top of the stem and determine the bending moment and shear force distribution over the height of the stem. This can be expressed as

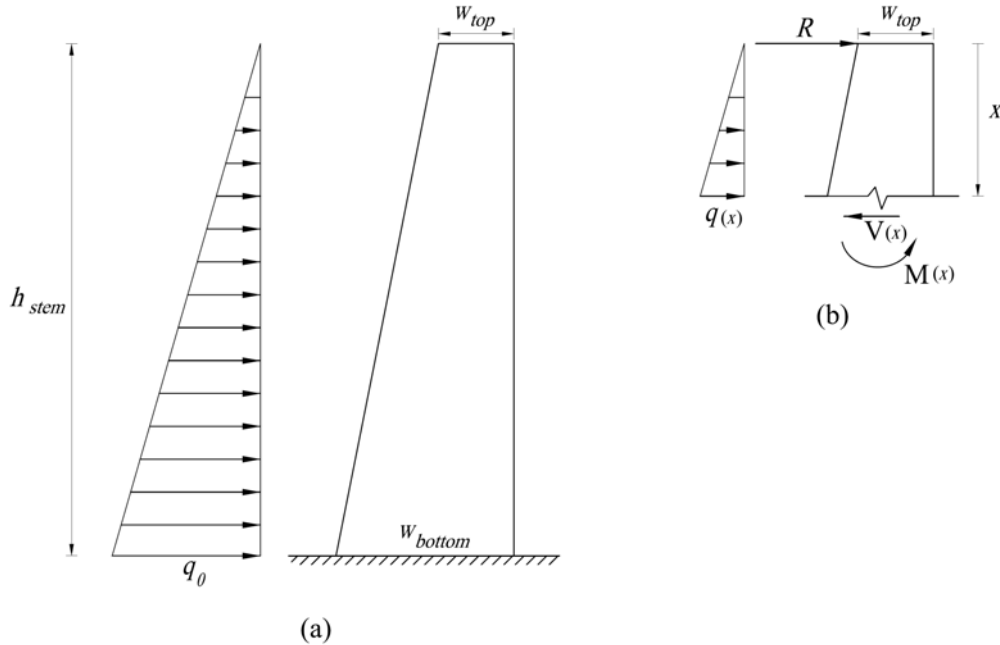


Fig. 4 Calculation of the stem deflection at the top using the Castigliano's second theorem

$$\delta_b = \int_0^{h_{stem}} \frac{M(x)}{EI(x)} \times \frac{\partial M(x)}{\partial R} dx \quad (17)$$

$$\delta_s = \int_0^{h_{stem}} \frac{\alpha V(x)}{GA(x)} \times \frac{\partial V(x)}{\partial R} dx \quad (18)$$

where  $\delta_b$  and  $\delta_s$  are the deflection at the top of the stem due to flexure and shear, obviously the total deflection is obtained by summing up the values of these two parameters.  $E$  is the modulus of elasticity and  $G$  is the shear modulus.  $R$  represents the dummy force and  $\alpha$  is the shear shape factor of the cross section. By calculating the area and the moment of inertia of the cross-section as well as the bending moment and the shear at a distance  $x$  from the top, and substituting them in the above equations, we obtain

$$\delta_b = \frac{q_0 h_{stem}^4}{6EI_0 k^5} \left\{ \frac{k^4 - 4k^3 - 18k^2 - 12k}{2(k+1)^2} + 6Ln(k+1) \right\} \quad (19)$$

$$\delta_s = \frac{3q_0 h_{stem}^2}{5GA_0 k^3} \left\{ \frac{k^2 - 2k}{2} + Ln(k+1) \right\} \quad (20)$$

where  $A_0$  and  $I_0$  are the area and the moment of inertia of the cross-section at the top of the stem per meter length of the wall and  $k$  is a dimensionless parameter given by  $k = (w_{bottom} - w_{top}) / w_{top}$ .

## 5. Metaheuristic algorithm: NSGA-II

In the following, a general description of the NSGA-II will be presented. The algorithm and its detailed implementation procedure can be found in Deb (2009). Once the population is initialized, two fitness values are assigned to each individual. Firstly, the NSGA-II uses a “non-dominated sorting” algorithm for the fitness assignment, in which all individuals not dominated by any other individuals, are assigned front number 1. Then all individuals only dominated by individuals in front number 1 are assigned front number 2, and so on. Secondly, a value called “crowding distance” is calculated for each individual that is a measure of how close an individual is to its neighbors. A higher fitness value is assigned to individuals located on the sparsely populated part of a front.

Parent selection is made using a “binary tournament selection” based on the assigned fitness values. This selects, between two random individuals, the one with the lowest front number, if the two individuals are from different fronts. While the individuals are from the same front, the individual with the highest crowding distance is chosen. Next, the selected individuals generate offsprings using the genetic operators. The offspring population is combined with the current generation’s population and replacement is performed to set the individuals of the next generation. Since all the previous and current best individuals are included, elitism is ensured. The combined population is now sorted based on the non-domination rule. The new generation is filled by each front subsequently until the population size exceeds the given size. If by adding all the individuals from the  $i$ th front, the population size exceeds, then individuals in the  $i$ th front are selected based on their crowding distance in the descending order until the population is fulfilled. And hence, this process repeats to generate the subsequent generations, until the termination criteria is met.

### 5.1 Genetic operators

The chosen genetic operators are the well-known 1-point crossover and a modified version of polynomial mutation developed to solve our integer-valued problem. The role of crossover operator is to inherit some genetic materials of two parents to generate the offsprings whereas mutation alters one or more gene values in a chromosome from its initial state. Hence, the mutation and crossover operators are complementary, that is, mutation maintains genetic diversity from one generation of a population of algorithm chromosomes to the next while the crossover operator preserves the heritability between generations (Talbi 2009).

In the 1-point crossover, a crossover point is randomly selected at the same position in the two individuals, and then two offsprings are created by interchanging all the information of the parents positioned after this cut point in their chromosomes. Thus the new individuals have information from the two initial individuals but they are different. In general, a uniform random distribution is used to select the crossover point (Talbi 2009). After the crossover operator is performed, mutation takes place on the newly formed individuals.

In the polynomial mutation, which was originally introduced for real-valued optimization, the offspring is generated as follows (Talbi 2009)

$$x'_i = x_i + (x_i'' - x_i')\delta_i \quad (21)$$

where  $x_i''$  (resp.  $x_i'$ ) represents the upper bound (resp. lower bound) for  $x_i$ , the  $i$ th variable (gene) of parent. The parameter  $\delta_i$  is computed from the following polynomial probability distribution:

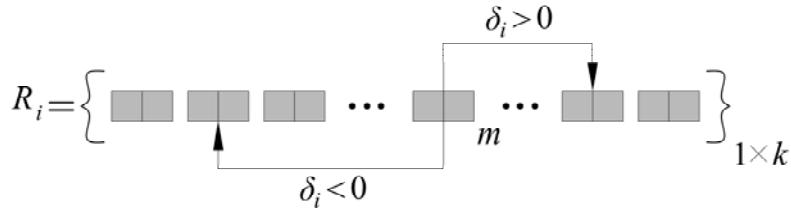


Fig. 5 Discrete polynomial mutation of the  $i$ th gene

$$\delta_i = \begin{cases} (2r_i)^{\frac{1}{\eta_m+1}} - 1 & \text{if } r_i < 0.5 \\ 1 - (2(1-r_i))^{\frac{1}{\eta_m+1}} & \text{otherwise} \end{cases} \quad (22)$$

where  $\eta_m$  denotes the distribution index and  $r_i$  is a random number in  $[0, 1]$ . Mutation should produce a minimal change and the size of mutation should be controllable. The parameter  $\eta_m$  provides these features, e.g., taking  $\eta_m$  to be 5, limits the values of  $\delta_i$  in  $[-0.4, 0.4]$ .

Mutation in discrete representation consists generally in changing the value associated with a variable by a new value from the vector of allowable values. In this paper, we have utilized the polynomial probability distribution in determining the new value of the mutation. This procedure is schematically depicted in Fig. 5. As is shown, based on the value generated by Eq. (22), a value is selected among the values are on the left side of the current value in the vector (when  $\delta_i < 0$ ), or among the values are on the right side (when  $\delta_i > 0$ ). Considering two portions for each value, the probability of choosing a value from the left side is  $2/(2(m-1)+1)$ , and from the right side  $2/(2(k-1)+1)$ , where  $m$  defines the position of the current value and  $k$  is the size of the vector. Hence, the new value is obtained by

$$\begin{cases} \left\{ \begin{aligned} s &= \frac{1}{2(m-1)+1} \\ t &= \left\lfloor \frac{abs(\delta_i) + s}{2s} \right\rfloor \\ x'_i &= R_i(m-t) \end{aligned} \right. & \text{if } \delta_i < 0 \\ \left\{ \begin{aligned} s &= \frac{1}{2(k-m)+1} \\ t &= \left\lfloor \frac{\delta_i + s}{2s} \right\rfloor \\ x'_i &= R_i(m+t) \end{aligned} \right. & \text{otherwise} \end{cases} \quad (23)$$

where  $R_i$  is the vector of allowable values for the  $i$ th gene.

## 5.2 Constraint handling

In order to handle the given constraints, a relatively simple scheme is adopted. Whenever two individuals are compared, for sorting the population in different fronts, first, they are checked for constraint violation. If both are feasible, the non-domination rule is directly applied to decide the winner. If one is feasible and the other is unfeasible, the feasible dominates. If both are unfeasible, then the one with the lowest amount of constraint violation dominates the other. This is the approach that has been utilized in (Deb *et al.* 2002, Coello *et al.* 2004) to handle the constraints.

## 6. The proposed framework

Now, all of the introduced components in the previous sections are incorporated in a simple framework, which makes it possible to perform the multi-objective optimal design of retaining walls. The main procedure, which is based on the NSGA-II genetic algorithm, is as follows. The relevant section to some steps are noted in brackets:

*Main procedure* {

1. Set parameters.
  - 1.1. Set the NSGA-II user defined parameters, *e.g.*, population size, number of parents, number of offsprings, number of generations, *etc.*
  - 1.2. Structural modeling [Sect. 3].
2. Initialize the population.
  - 2.1. Generate a random individual.
  - 2.2. Perform structural evaluation module [Sect. 4].
  - 2.3. Calculate the constraint violation.
  - 2.4. Evaluate the objective functions [Sect. 2].
3. Sort the initial population based on the constraint handling rule [Sect. 5.2].
4. Until termination criterion met.
  - 4.1. Select parents using binary tournament selection.
  - 4.2. Generate offsprings by performing crossover and mutation operators [Sect. 5.1].
    - 4.2.1. Generate a new individual.
    - 4.2.2. Perform structural evaluation module [Sect. 4].
    - 4.2.3. Calculate the constraint violation.
    - 4.2.4. Evaluate the objective functions [Sect. 2].
  - 4.3. Form an intermediate population from merging the current population with the offsprings.
  - 4.4. Sort the intermediate population based on the constraint handling rule [Sect. 5.2].
  - 4.5. Perform replacement on the intermediate population to determine the new population.

}.

## 7. Numerical results

The proposed framework is implemented in MATLAB<sup>®</sup> and a program is developed for contractibility optimal design of RC retaining walls. As a test problem, design of a typical wall of 8 m in height and 100 m in length is studied in this section. Details of the parameters assumed in

Table 2 Parameters of the reported retaining wall.

| Parameter   | Value                  |
|---|------------------------|
| Top thickness of the stem ( $w_{top}$ )                       | 0.5 m                  |
| Height of soil on the toe ( $h_{front}$ )                     | 0.8 m                  |
| Surcharge load ( $\omega$ )                                   | 1000 kg/m <sup>2</sup> |
| Backfill slope ( $i$ )  | 0°                     |
| Internal friction angle of backfill ( $\phi$ )                | 30°                    |
| Friction angle between stem and backfill ( $\delta$ )         | 0°                     |
| Internal friction of foundation soil ( $\phi$ )               | 30°                    |
| Friction angle between base and foundation soil ( $\delta'$ ) | 24°                    |
| Inclination of backfill pressure                              | 0°                     |
| Allowable ground stress ( $q_a$ )                             | 3.5 kg/cm <sup>2</sup> |
| Unit weight of backfill ( $\gamma_{soil}$ )                   | 1850 kg/m <sup>2</sup> |
| Unit weight of concrete ( $\gamma_{conc}$ )                   | 2400 kg/m <sup>2</sup> |
| Overturning safety factor                                     | 1.5                    |
| Sliding safety factor   | 1.125                  |
| Bearing capacity safety factor                                | 1.5                    |
| Allowable stem deflection                                     | 1/150 $h_{stem}$       |

this example are listed in Table 2. The reported partial safety factors are in accordance with AASHTO (2002), which permits the factors of safety against sliding and overturning failure under seismic loading reduced to 75% of the factors of safety used for the static loading designs. The specified yield strength of flexural reinforcement is considered to be 4000 kg/cm<sup>2</sup> and for the shear reinforcement is taken as 3000 kg/cm<sup>2</sup>.

In order to achieve a more precise cost evaluation of the wall, both the development and anchorage length are added to the required length of the bars wherever needed, according to the ACI 318-08 provisions. In this paper, the entire search takes place in a discrete decision space. The allowable values considered for the design variables, and their lower and upper bounds are summarized in Table 3. It should be noted that if the depth of the shear key is obtained to be less than 0.5 m, the shear key is omitted and all the design variables assigned to the shear key are considered to be zeros.

The present study tries to enhance constructability by using practical reinforcement arrangements and ensuring that bar spacing satisfies the design code limitations. ACI 318-08 contains detailed provisions for determining spacing limits between reinforcement bars. The values considered in this study for the allowable maximum and minimum clear spacing between parallel flexural bars in a layer, or spacing of shear reinforcement placed perpendicular to axis of member, reported in Table 3, last two rows, covers the requirements of ACI 318-08.

In order to investigate how much the considered objective functions are in conflict with each other, a random search was performed with 100,000 iterations, including both feasible and unfeasible solutions. Fig. 6 depicts the linear regression of the cost on the number of bars for the obtained solutions. The low determination coefficient of  $R^2 = 0.2048$  indicates that the objectives are quite independent. The percentage of feasible solutions is 0.15%, which means only about one and half in a thousand randomly generated solutions are feasible. This low percentage shows that the optimization problem is highly constrained

Table 3 Allowable values of the design variables

| Description           | Allowable value  | Unit |
|-----------------------|--|------|
| $f_c$                 | {20, 25, 30, 35, 40}                                     | MPa  |
| $w_{bottom}$          | $[w_{top} + 0.02 \times h_{stem}; 0.2 : 3]^*$            | m    |
| $h_{slab}$            | [0.6 : 0.2 : 3]  | m    |
| $w_{heel}$            | [0 : 0.2 : $h_{stem}$ ]                                  | m    |
| $w_{toe}$             | [0 : 0.2 : $h_{stem}$ ]                                  | m    |
| $h_{key}$             | [0 : 0.2 : 3]  | m    |
| $w_{key}$             | [0 : 0.2 : 2]  | m    |
| $b_{key}$             | [0 : 0.2 : $w_{heel} + w_{bottom} + w_{toe} - w_{key}$ ] | m    |
| Flexural bar diameter | {16, 18, 20, 22, 25, 26, 28, 30, 32}                     | mm   |
| Shear bar diameter    | {6, 8, 10, 12}   | mm   |
| Flexural bar spacing  | $[D_i^{**} + 5; 5 : 30]$                                 | cm   |
| Shear bar spacing     | $[D_i + 5; 5 : 30]$                                      | cm   |

\*Generates values from the lower to the upper bound with a constant step size (the middle value).

\*\*Denotes the diameter of the  $i$ th reinforcement set.

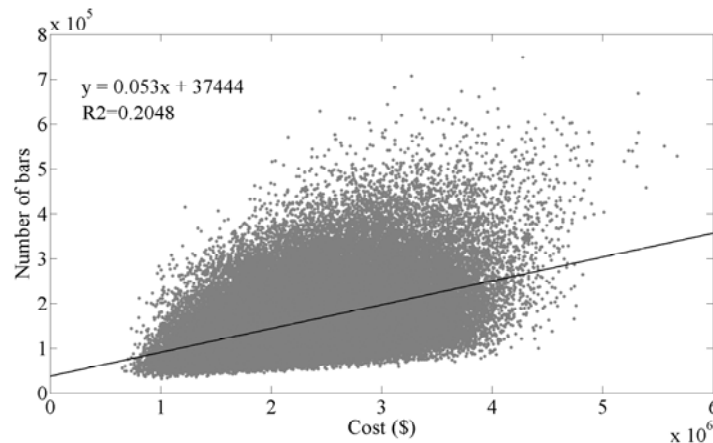


Fig. 6 Linear regression of the cost on the number of bars

Because of the stochastic nature of the solution algorithm, this problem was solved 6 times. The obtained Pareto fronts are shown in Fig. 7. In this example, a population of 1000 individuals is employed for optimization process and the main algorithm performs 150 generations. The computational time required for solving this problem using the developed program was approximately 1.4 h on an Intel® Core™ i7 @ 2.0 GHz processor equipped with 8 GBs of RAM, for each run.

In order to compare the properties of the different optimal designs achieved in the shown Pareto fronts, two characteristic designs are investigated. These designs are the extreme points corresponding to the single-objective optimal designs where the economic cost and the number of bars are the objective functions, i.e., the designs with minimum cost and minimum reinforcing bar congestion. The properties of these two designs are listed in Table 4. As is presented, while the cost of design B compared to design A is increased by 32.6%, the corresponding reinforcing bar congestion is decreased by 40.7%.

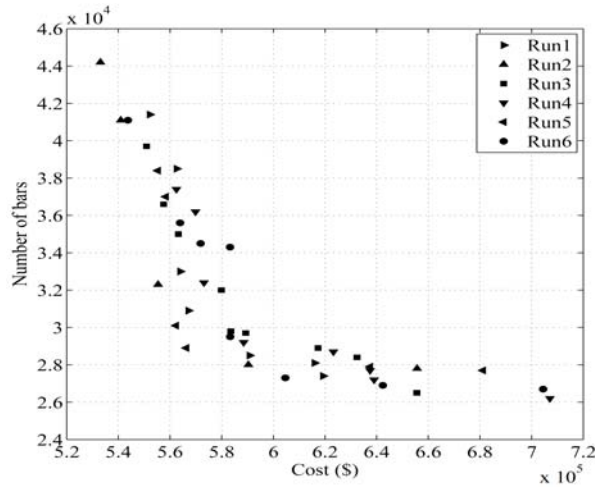


Fig. 7 Pareto fronts obtained in six different runs for the reported retaining wall

Table 4 Properties of two characteristic designs of the reported retaining wall

| Optimal design variables    |                  |                |             |                  |                 |                        |          |         |   |          |          |
|-----------------------------|------------------|----------------|-------------|------------------|-----------------|------------------------|----------|---------|---|----------|----------|
| No.                         | Design variable* | Design A**     | Design B*** | No.              | Design variable | Design A               | Design B | No.     | Design variable                                       | Design A | Design B |
| 1                           | $w_{bottom}$     | 0.86           | 1.26        | 14               | $D_5$           | 18                     | 22       | 27      | $S_3$   | 23       | 22       |
| 2                           | $h_{slab}$       | 0.60           | 1.00        | 15               | $D_6$           | 30                     | 22       | 28      | $S_4$   | 17       | 27       |
| 3                           | $w_{heel}$       | 1.60           | 4.20        | 16               | $D_7$           | 18                     | 20       | 29      | $S_5$   | 23       | 23       |
| 4                           | $w_{toe}$        | 4.60           | 2.00        | 17               | $D_8$           | 16                     | 30       | 30      | $S_6$   | 13       | 18       |
| 5                           | $h_{key}$        | 1.00           | 0.00        | 18               | $D_9$           | 18                     | 32       | 31      | $S_7$   | 16       | 26       |
| 6                           | $w_{key}$        | 0.40           | 0.00        | 19               | $D_{10}$        | 30                     | 22       | 32      | $S_8$   | 22       | 27       |
| 7                           | $b_{key}$        | 4.60           | 0.00        | 20               | $D_{11}$        | 25                     | 32       | 33      | $S_9$   | 28       | 0        |
| 8                           | $f_c(stem)$      | 25             | 25          | 21               | $D_{12}$        | 30                     | 18       | 34      | Number of shear bars in stem per meter length of wall | 4        | 3        |
| 9                           | $f_c(base)$      | 30             | 30          | 22               | $D_{13}$        | 8                      | 12       |         |   |          |          |
| 10                          | $D_1$            | 20             | 32          | 23               | $D_{14}$        | 16                     | 18       |         |   |          |          |
| 11                          | $D_2$            | 26             | 28          | 24               | $D_{15}$        | 32                     | 0        | 35      | Number of shear bars in base per meter length of wall | 3        | 3        |
| 12                          | $D_3$            | 20             | 22          | 25               | $S_1$           | 18                     | 28       |         |   |          |          |
| 13                          | $D_4$            | 10             | 8           | 26               | $S_2$           | 16                     | 26       |         |   |          |          |
| Fitness function evaluation |                  |                |             |                  |                 |                        |          |         |   |          |          |
|                             | Cost (\$)        | Number of bars |             | Cost improvement |                 | Congestion improvement |          |         |   |          |          |
|                             | Design A         | 533046         |             | 44200            |                 | 24.61%                 |          | -68.70% |   |          |          |
|                             | Design B         | 707053         |             | 26200            |                 | -32.64%                |          | 40.72%  |   |          |          |

\*Units are in accordance with Table 3

\*\*Indicates the design with minimum cost

\*\*\*Indicates the design with minimum reinforcing bar congestion

## 8. Conclusions

A multi-objective framework is proposed for constructability optimal design of RC retaining walls considering minimization of the economic cost and the reinforcing bar congestion as two objectives of the optimization problem. An advanced model of structure with 35 design variables is presented, including seven geometric, two material types, and 26 variables for reinforcement setup. The seismic response of the walls is investigated during the analysis process in accordance with the AASHTO provisions. NSGA-II genetic algorithm is employed as the optimization algorithm, equipped with a new version of polynomial mutation formulated for discrete representation. In this study, we have tried to consider all the relevant constraints included in the guidelines and practical matters in a way that the results can be useful for the engineers in real-life projects.

A computer program is developed based on the proposed framework and operated for the design of an RC retaining wall of 8 m in height and 100 m in length. As was reported, optimization of such structures based only on the cost tends to the reinforcement arrangements with close spacings of small diameter bars and poor constructability. Therefore, obtaining the Pareto front of all the possible optimal designs for these two objectives provides invaluable information that helps designers and investors to make the best decisions. This problem is specifically more involved in large-scale construction projects. It is demonstrated that by the use of the proposed framework, the constructability optimal design of RC retaining walls can be performed within acceptable amount of time while providing a convenient Pareto front of possible optimal designs.

## Acknowledgements

The first author is grateful to the Iran National Science Foundation for the support.

## References

- American Association of State Highway and Transportation Officials (AASHTO) (2002), *Standard Specifications for Highway Bridges*, 17th Edition, Washington, D.C.
- American Concrete Institute, committee 318 (ACI 318-08) (2008), *Building Code Requirements for Structural Concrete and Commentary*, Farmington Hills.
- Ceranic, B., Fryer, C. and Baines, R.W. (2001), "An application of simulated annealing to the optimum design of reinforced concrete retaining structures", *Comput. Struct.*, **79**(17), 1569-1581.
- Coello, C.A.C., Pulido, G.T. and Lechuga, M.S. (2004). "Handling multiple objectives with particle swarm optimization", *IEEE Trans. Evol. Comput.*, **8**(3), 256-279.
- Das, B.M. (2010), *Principles of Foundation Engineering*, 7th Edition, Cengage Learning, USA.
- Das, B.M. and Ramana, G.V. (2010), *Principles of Soil Dynamics*, 2nd Edition, Cengage Learning, USA.
- Deb, K., Pratap, A., Agarwal, S., Agarwal, S. and Meyarivan, T. (2002). "A fast and elitist multiobjective genetic algorithm: NSGA-II", *IEEE. Trans. Evolut. Comput.*, **6**(2), 182-197.
- Deb, K. (2009), *Multi-Objective Optimization Using Evolutionary Algorithms*, Wiley, New York, USA.
- Giri, D. (2011), "Pseudo-dynamic approach of seismic earth pressure behind cantilever retaining wall with inclined backfill surface", *Geomech. Eng.*, **3**(4), 255-266.
- Kaveh, A. (2006), *Optimal Structural Analysis*, 2nd Edition, John Wiley & Sons, UK.

- Kaveh, A. and Shakouri-Mahmud-Abadi, A. (2010), "Harmony search based algorithms for the optimum cost design of reinforced concrete cantilever retaining walls", *Int. J. Civil Eng.*, **9**(1), 1-8.
- Kaveh, A., Laknejadi, K. and Alinejad, B. (2011), "Performance-based multi-objective optimization of large steel structures", *Acta Mech.*, **223**(2), 355-369.
- Kaveh, A. and Behnam, A.F. (2012), "Charged system search algorithm for the optimum cost design of reinforced concrete cantilever retaining walls", *Arab. J. Sci. Eng.*, **37**(7), 1-8.
- Khajehzadeh, M., Taha, M.R. and Eslami, M. (2013), "Efficient gravitational search algorithm for optimum design of retaining walls", *Struct. Eng. Mech.*, **45**(1), 111-127.
- Martinez-Martin, F.J., Gonzalez-Vidoso, F., Hospitaler, A., Yepes, V. (2012). "Multi-objective optimization design of bridge piers with hybrid heuristic algorithms", *J. Zhejiang Univ. Sci. A (Appl. Phys. & Eng.)*, **13**(6), 420-432.
- MATLAB (2012), *The Language of Technical Computing*, Math Works Inc.
- Mononobe, N. (1929), "Earthquake-proof construction of masonry dams," *Proceedings of World Engineering Conference*, **9**, 274-280.
- Okabe, S. (1926), "General theory of earth pressure", *J. Jpn. Soc. Civ. Engrs.*, **12**(1).
- Saribas, A. and Erbatur, F. (1996). "Optimization and sensitivity of retaining structures" *J. Geotech. Eng. Div.*, **122**(8), 649-656.
- Talbi, E.G. (2009), *Metaheuristics: From Design to Implementation*, Wiley, New Jersey.
- Yepes, V., Alcalá, J., Perea, C. and Gonzalez-Vidoso, F. (2008), "A parametric study of optimum earth-retaining walls by simulated annealing", *Eng. Struct.*, **30**(3), 821-830.
- Yepes, V., Gonzalez-Vidoso, F., Alcalá, J. and Villalba, P. (2012), "CO<sub>2</sub>-optimization design of reinforced concrete retaining walls based on a VNS-threshold acceptance strategy", *J. Comput. Civ. Eng.*, **26**(3), 378-386.